

UTHEP-98-0502

May 1998

Final State Radiative Effects for the Exact $\mathcal{O}(\alpha)$ YFS Exponentiated (Un)Stable W^+W^- Production At and Beyond LEP2 Energies[†]

S. Jadach

*Institute of Nuclear Physics, ul. Kawiorów 26a, Kraków, Poland
CERN, Theory Division, CH-1211 Geneva 23, Switzerland,*

W. Płaczek

*Institute of Computer Science, Jagellonian University, Kraków, Poland
CERN, Theory Division, CH-1211 Geneva 23, Switzerland,*

M. Skrzypek

*Institute of Nuclear Physics, ul. Kawiorów 26a, Kraków, Poland
CERN, Theory Division, CH-1211 Geneva 23, Switzerland,*

B.F.L. Ward

*Department of Physics and Astronomy,
The University of Tennessee, Knoxville, Tennessee 37996-1200
SLAC, Stanford University, Stanford, California 94309
CERN, Theory Division, CH-1211 Geneva 23, Switzerland,*

Z. Wąs

*Institute of Nuclear Physics, ul. Kawiorów 26a, Kraków, Poland
CERN, Theory Division, CH-1211 Geneva 23, Switzerland*

Abstract

We present the LL final state radiative effects for the exact $\mathcal{O}(\alpha)$ YFS exponentiated (un)stable WW pair production at LEP2/NLC energies using Monte Carlo event generator methods. The respective event generator, version 1.12 of the program YFSWW3, wherein both Standard Model and anomalous triple gauge boson couplings are allowed, generates $n(\gamma)$ radiation both from the initial state and from the intermediate W^+W^- and generates the LL final state W decay radiative effects. Sample Monte Carlo data are illustrated.

To be submitted to Physical Review D

[†] Work partly supported by the Polish Government grants KBN 2P30225206 and 2P03B17210 and by the US Department of Energy Contracts DE-FG05-91ER40627 and DE-AC03-76ER00515.

UTHEP-98-0502

May, 1998

The role of the final state radiative (FSR) effects in the processes $e^+e^- \rightarrow W^+W^- + n(\gamma) \rightarrow 4f + n(\gamma)$ at and beyond LEP2 energies is of considerable interest for the LEP2 and NLC physics programs [1, 2, 3]. In this paper, we evaluate for the first time, the possible interplay between the exact $\mathcal{O}(\alpha)$ electroweak (EW) corrections and the leading-log (LL) final-state radiative effects for these processes when the $n(\gamma)$ radiation is realized according to the amplitude based Monte Carlo event generator techniques in Ref. [4, 5], wherein infrared singularities are cancelled to all orders in α using the extension to spin 1 charged particles of the theory of Yennie, Frautschi and Suura for QED in Ref. [6].

The final state radiative effects are realized in the LL approximation using the calculation of the program PHOTOS in Ref. [7] in which a non-radiative final state process is used to generate up to two photons in the corresponding radiative process by iterating the structure function evolution equation¹ for QED [8]. The exact $\mathcal{O}(\alpha)$ YFS exponentiated final state W decay radiative effects will appear elsewhere [9]. In this connection, we note that we expect the non-leading $\mathcal{O}(\alpha)$ and higher order ($\mathcal{O}(\alpha^n)$, $n \geq 2$) final state radiative effects to be small, $\sim 1\%$ in the peak reduction effect [2] for example, even for a “bare trigger” acceptance for the outgoing final charged particles. This has been found by the authors in Ref. [2], who analysed the effects of final state radiation in Z decay in the naive exponentiated (exact and LL) $\mathcal{O}(\alpha)$ approximation and who estimated the corresponding size of the analogous effects in W decay as $\sim 14\%$ for the total peak reduction effect for example. Indeed, more recently, the authors in Ref. [2] have made an independent cross check on their estimates of the FSR line shape effects for $e^+e^- \rightarrow W^+W^- \rightarrow 4f$ in Ref. [3], wherein they present an exact $\mathcal{O}(\alpha)$ calculation of the process in the double pole approximation (DPA) in which one retains in the pole expansion [10] of the complete $e^+e^- \rightarrow 4f$ amplitude only the terms containing the double pole in the S-matrix at the complex mass squared $M^2 = M_W^2 - iM_W\Gamma_W$ where M_W, Γ_W are the respective mass and width of the W boson. and where in the residues of the respective double poles one projects the respective $\mathcal{O}(\alpha)$ corrections to an appropriate on-shell point. Henceforth, we refer to the on-shell residue projected DPA as the leading pole approximation (LPA) with more general applications in mind: for example, in a triply resonant process, the LPA would correspond to the triple pole terms in the respective S-matrix element with the residues projected to an appropriate on-shell point. In this gauge invariant calculation, these authors find that the FSR peak reduction effect is $\sim 14.4\%$ for $W^{+(-)} \rightarrow e^{+(-)}\nu_e(\bar{\nu}_e)$ to be compared with their estimate in Ref. [2] of $\sim 14\%$. We will compare our results with those in Refs. [2, 3]. We emphasise that our work differs from the work on Ref. [2] in that we include the exact EW $\mathcal{O}(\alpha)$ corrections with YFS exponentiation in the production process and we actually calculate the effects of the FSR in the W -pair production and decay process at LEP2/NLC energies whereas in Ref. [2] only the process $\nu_\mu\bar{\nu}_\mu \rightarrow ZZ \rightarrow e^+e^- + \nu_\tau\bar{\nu}_\tau$ is actually calculated and a heuristic argument is used to estimate corresponding results for final state W -decay radiation. Thus, our calculations will also comment on the accuracy

¹To be precise an ansatz is provided which reproduces the LL terms. It includes transverse degrees of freedom for the photon 4-momentum, assures coverage of the full phase space and rules of energy-momentum conservation. The photons’ angular distribution is chosen to reproduce exactly the one of the soft photon limit. See the reference for more details.

of these heuristic arguments in the presence of the YFS exponentiated exact $\mathcal{O}(\alpha)$ corrections to the W -pair production process. Our work differs from that in Ref. [3] in that we include the YFS exponentiation of the exact $\mathcal{O}(\alpha)$ production process in the W -pair intermediate state and the $\mathcal{O}(\alpha)^2$ LL FSR whereas in Ref. [3], the exact $\mathcal{O}(\alpha)$ correction to the production and decay processes for the W -pair in the leading pole approximation is calculated without exponentiation, wherein the leading pole approximation treatment of the attendant nonfactorizable corrections in Refs. [11, 12, 14] is also retained. The latter non-factorizable corrections have been shown [11, 12, 14] to be small and, as we explain Ref. [5], when one works up to but not including $\mathcal{O}(\frac{\alpha}{\pi} \frac{\Gamma_W}{M_W})$ as we do, such effects may be dropped and we do this. Thus, although we start our calculation in Ref. [5] in the fermion-loop scheme [15], when we focus on the $\mathcal{O}(\alpha)$ EW virtual correction, we go to the leading pole part of the respective production amplitude and make the approximation of using on-shell residues for this double pole part, which we then use to approximate the respective $\mathcal{O}(\alpha)$ EW correction. In our Monte Carlo event generator approach, we stress that the full off-shell phase space is always retained here. We improve our result by using the complete on-shell residues for EW corrections rather than their on-shell fermion-loop scheme representatives. Indeed, for the QED bremsstrahlung correction we stress that, since the real photon has $k^2 = 0$, the respective running charge is the usual one and it can thus be shown that, in $\mathcal{O}(\alpha)$, the respective on-shell fermion-loop scheme bremsstrahlung residues are equivalent to those in the LPA and in both cases all IR singularities are properly cancelled and not only is the QED gauge invariance preserved but also the full $SU_{2L} \times U_1$ gauge invariance is preserved [4, 5]. For this reason, in order $\mathcal{O}(\alpha)$, in our final result, any reference to the fermion-loop scheme is purely pedagogical. What we arrive at is precisely the LPA with full on-shell residues for the respective double pole approximation. As one can see also from the results in Ref. [3], these approximations are valid up to but not including $\mathcal{O}(\frac{\alpha}{\pi} \frac{\Gamma_W}{M_W})$. We then apply our YFS Monte Carlo methods of two of us (S.J. and B.F.L.W.) [16], as extended to spin 1 particles in Ref. [4], to arrive at the respective exact $\mathcal{O}(\alpha)_{prod}$ YFS exponentiated results realized in YFSWW3-1.11. Hence, we stress that, as far as the $\mathcal{O}(\alpha)$ correction to the production process under study is concerned, the results in Ref. [3] and in Ref. [5] should be equivalent, in view of the many cross checks carried by the authors in Refs. [17, 18, 19] on the two respective electroweak on-shell calculations used therein.

More precisely, starting from the calculations in the program YFSWW3-1.11 in Ref. [5], which feature the exact $\mathcal{O}(\alpha)_{prod}$ YFS exponentiated results for the process $e^+e^- \rightarrow W^+W^- + n(\gamma) \rightarrow 4f + n(\gamma)$, we have interfaced the outgoing final state to the program PHOTOS [7], which uses the structure function evolution equation for QED [8] to add up to two final state decay photons to each W according to the respective LL probabilities to radiate, where the corresponding angular distributions of the decay photons are all generated in accordance with this LL approximation as it is described in Ref. [7]. The net probability of the respective event is unchanged, i.e., the normalisation of YFSWW3-1.11 is unaffected by this interface, which will be described in more detail elsewhere [9]. We refer to the version of YFSWW3 with this final state radiative interface to PHOTOS as YFSWW3-1.12 and it is available from the authors [13]. In what follows, we present some

sample Monte Carlo data from YFSWW3-1.12 to look into the possible role of FSR in the presence of the $\mathcal{O}(\alpha)$ EW corrections. For definiteness, we focus here on the current LEP2 CMS energy of 190GeV and on the SM couplings. The complete discussion of both LEP2 and NLC energies with the illustration of anomalous couplings will appear elsewhere [9].

Specifically, in Figs. 1–8, we show the results obtained with YFSWW3-1.12 for the processes $e^+e^- \rightarrow W^+W^- + n(\gamma) \rightarrow \bar{c}s + \ell\bar{\nu}_\ell$, $\ell = e, \mu$ for the cosine of W production angle distribution in the CM (LAB) system, for the W mass distribution, with both “bare” and “calorimetric” definitions of that mass, for the CMS lepton final energy distribution, for both calorimetric and bare definitions of that energy, and for the corresponding distributions of the cosine of the lepton decay angle in the W rest frame.

We note the following properties of these results. First, concerning the W mass distributions in Figs. 1 and 5, we see that the respective average values of M_W are as given in Table 1. Here, *EW-ex* denotes the exact $\mathcal{O}(\alpha)_{prod}$ [5] EW corrections calculation, *EW-ap* denotes the approximate treatment of these EW corrections as given in Ref. [20], and *No EW* denotes that the EW corrections other than the LL ($\mathcal{O}(\alpha^2)$) initial-state-radiation are turned-off.

E_{CM} [GeV]	Calculation	FSR	CUT	$\langle M_W \rangle$ [GeV]
		$W^- \rightarrow e^- \bar{\nu}_e$		
190	<i>Born</i>	–	<i>BARE</i>	80.253 ± 0.008
	<i>EW-ex</i>	<i>NO</i>	<i>BARE</i>	80.146 ± 0.036
	<i>No EW</i>	<i>NO</i>	<i>BARE</i>	80.142 ± 0.036
	<i>No EW</i>	<i>YES</i>	<i>BARE</i>	78.614 ± 0.035
	<i>EW-ap</i>	<i>YES</i>	<i>BARE</i>	78.613 ± 0.035
	<i>EW-ex</i>	<i>YES</i>	<i>BARE</i>	78.618 ± 0.035
	<i>No EW</i>	<i>YES</i>	<i>CALO</i>	79.727 ± 0.036
	<i>EW-ap</i>	<i>YES</i>	<i>CALO</i>	79.725 ± 0.036
	<i>EW-ex</i>	<i>YES</i>	<i>CALO</i>	79.731 ± 0.036
		$W^- \rightarrow \mu^- \bar{\nu}_\mu$		
190	<i>Born</i>	–	<i>BARE</i>	80.253 ± 0.008
	<i>EW-ex</i>	<i>NO</i>	<i>BARE</i>	80.146 ± 0.036
	<i>No EW</i>	<i>NO</i>	<i>BARE</i>	80.142 ± 0.036
	<i>No EW</i>	<i>YES</i>	<i>BARE</i>	79.374 ± 0.036
	<i>EW-ap</i>	<i>YES</i>	<i>BARE</i>	79.373 ± 0.036
	<i>EW-ex</i>	<i>YES</i>	<i>BARE</i>	79.378 ± 0.036
	<i>No EW</i>	<i>YES</i>	<i>CALO</i>	79.725 ± 0.036
	<i>EW-ap</i>	<i>YES</i>	<i>CALO</i>	79.724 ± 0.036
	<i>EW-ex</i>	<i>YES</i>	<i>CALO</i>	79.730 ± 0.036

Table 1: The results of the 125×10^6 statistics samples (weighted events) (except for *Born*, where the sample is 540×10^6 of such events) from YFSWW3-1.12 for the average value of M_W as computed with the levels of radiative corrections as indicated for both bare and calorimetric treatments of the final lepton. See the text for more details.

The calorimetric results are all closer to their respective *NO FSR* analogs than are the bare results, as expected. The effects of the FSR for the muon case are all respectively less than the corresponding results for the electron case, again as expected due to the smaller radiation probability for the muon. The size of the shift of $\langle M_W \rangle$ is generally consistent with the discussion in Ref. [2], which deals with the line shape (peak position and height) primarily, but we see in detail that, in the presence of the FSR, at the level of our statistical errors, for the average quantity such as $\langle M_W \rangle$, all three calculations in the table are sufficient, as expected. With regard to the guesstimates made in Ref. [2] concerning the peak reduction and the peak position shift, we see from our *BARE* curves in Fig. 1 that our result of 13.5% for the peak reduction for the e^- case (comparing the *EW-ex* curves with and without FSR) is in good agreement with the 14% guesstimated in Ref. [2] and with the 14.4% found in the recent $\mathcal{O}(\alpha)$ on-shell LPA results in Ref. [3]. The ~ -57 MeV guesstimated in Ref. [2] for the corresponding peak position shift in the e^- case has been updated recently in the Ref. [3] using calculations as already noted to -77 MeV; for the μ case, the updated expectation from Ref. [3] for the peak position shift is -39 MeV. For completeness, we note that the size of the peak reduction effect in the μ case has been found to be $\sim 8\%$ in Ref. [3] whereas in Fig. 5 we find this latter effect to be 7.6%, again showing good agreement between our results and those in Ref. [3]. Indeed, to compare our results for the peak position shift with those just cited from Ref. [3], we have performed Breit-Wigner fits to our line shapes in Figs. 1 and 5 with the width of the W both fixed and floating. The results of our fits are shown in Table 2.

For comparison, the fits are done for two different mass intervals, from 78 GeV to 82 GeV, and from 76 GeV to 84 GeV, to illustrate role of the wings of the resonance in the fits. From these results we find that the BARE peak position shifts are estimated using the narrow fit range as $80.168 - 80.240 = -72$ MeV and $80.199 - 80.241 = -42$ MeV for the e and μ cases, respectively. We also computed the shift in the average invariant mass $\langle M_W \rangle$ of the W in the narrow range from 78 GeV to 82 GeV as another estimate of the peak position shift for the BARE trigger and we found -81.5 ± 1.4 MeV and -43.9 ± 0.9 MeV, respectively, for the e and μ cases. Thus, both sets of estimators of the peak position shifts are in reasonable agreement with the results in Ref. [3]², where we recall the slight difference in beam energy of our studies (95 GeV) vs those in Ref. [3] (92 GeV) in this connection. Moreover, we see in Table 2 the same pattern of results as we see in Table 1: the FSR effects for the e case are more pronounced than those for the μ case; the calorimetric acceptance reduces the size of the FSR effects; and, the results are not very sensitive to the EW correction to the production process. If one compares the predictions with and without FSR for the *EW-ex* and *no EW* cases one gets a measure of the modulation of the FSR on the EW correction. From the curves in our Figs. 1 and 5 and the respective plots of the δ_{RAD} as defined in the figures we see that this modulation is as expected. Concerning the cosine of the W production angle distributions, we see the interplay of the exact EW corrections on the one hand and the FSR on the other. We see further that

² The fit mass shift and the peak position shift approach one another as the fit range approaches a zero size interval around the peak; a similar remark applies to the shift in the average mass relative to the range over which it is taken around the peak.

M_W or M_W/Γ_W [GeV]							
$W^- \rightarrow e^- \bar{\nu}_e$							
	M -range [GeV]	<i>No FSR</i>		<i>FSR-BARE</i>		<i>FSR-CALO</i>	
		Γ_W -fix	Γ_W -fit	Γ_W -fix	Γ_W -fit	Γ_W -fix	Γ_W -fit
<i>Born</i>	78 – 82	80.240	80.240/2.0413				
	76 – 84	80.239	80.239/2.0376				
<i>No EW</i>	78 – 82	80.231	80.231/2.0442	80.166	80.168/2.2105	80.216	80.217/2.0831
	76 – 84	80.227	80.227/2.0372	80.142	80.135/2.2547	80.207	80.207/2.0892
<i>EW-ap</i>	78 – 82			80.166	80.168/2.2105	80.216	80.217/2.0832
	76 – 84			80.142	80.134/2.2547	80.207	80.207/2.0892
<i>EW-ex</i>	78 – 82	80.231	80.231/2.0443	80.166	80.168/2.2105	80.216	80.217/2.0832
	76 – 84	80.227	80.227/2.0372	80.142	80.134/2.2547	80.207	80.207/2.0892
$W^- \rightarrow \mu^- \bar{\nu}_\mu$							
<i>Born</i>	78 – 82	80.241	80.241/2.0308				
	76 – 84	80.250	80.250/2.0295				
<i>No EW</i>	78 – 82	80.232	80.232/2.0342	80.198	80.199/2.1196	80.217	80.218/2.0731
	76 – 84	80.238	80.238/2.0307	80.192	80.190/2.1481	80.217	80.217/2.0845
<i>EW-ap</i>	78 – 82			80.198	80.199/2.1196	80.217	80.218/2.0731
	76 – 84			80.192	80.190/2.1481	80.217	80.217/2.0845
<i>EW-ex</i>	78 – 82	80.232	80.232/2.0343	80.198	80.199/2.1196	80.217	80.218/2.0731
	76 – 84	80.238	80.238/2.0307	80.192	80.190/2.1481	80.217	80.217/2.0845

Table 2: The results of the Breit-Wigner line shape fit to the YFSWW3-1.12 MC sample for the W^- invariant mass distribution at $E_{CMS} = 190$ GeV. The input values of the W mass and width were: $M_W = 80.23$ GeV and $\Gamma_W = 2.03367033$ GeV (this value was used in the Γ_W -fix fit). The fits were performed for two W invariant mass M ranges – as indicated in the table. See the text for more details.

the approximate EW corrections of Ref. [20], while a definite improvement compared to no EW corrections at all, are not sufficient to describe this interplay at the level of 0.5–1.0%. Similar remarks hold for the lepton energy distribution in the CM system, although the respective insufficiency is reduced to the level of $\sim 0.3\%$ for the *BARE* case for example for electrons. Concerning the lepton decay angle cosine distributions in the W rest frame, we again see the importance of including both the EW corrections and the FSR in Figs. 4 and 8 for the electron and the muon respectively. In all cases, the results for the muon, particularly the *BARE* results, are less affected by the FSR than are the corresponding results for the electron, as expected. We stress that our results in Figs. 1–8 are generally consistent with those in Ref. [3] when one remembers that we treat the $\mathcal{O}(\alpha^2)$ LL FSR and the YFS exponentiated on-shell exact $\mathcal{O}(\alpha)_{prod}$ production process whereas Ref. [3] treats only $\mathcal{O}(\alpha)$ corrections in our LPA in which only on-shell residues are used. Indeed, in addition to the agreements already cited, we call attention to the normalisation correction in Fig. 9 of Ref. [3]: at the CMS energy $\sqrt{s} = 190$ GeV, it is -11% , in very good agreement with our result from Ref. [5] which is $(1 + \delta_{prod})(\rho_w)^2 - 1 \cong -11.1\%$, where we have used Table 2 in Ref. [5] for the relative correction $\delta_{prod} = -9.9\%$ to the production process and the result in Ref. [21] for the $\mathcal{O}(\alpha)$ correction to the leptonic partial width $\rho_w - 1 \cong -0.686\%$. In addition, we can note that, for the case of $\tau \bar{\nu}_\tau$ decay channel,

our results are also consistent with those in Ref. [3] for the peak position shift and peak reduction effects. In view of our higher order corrections, we find all of the agreements here noted quite reasonable. More detailed discussion of such comparisons will appear elsewhere [9]. We stress that we have arrived at our results via a MC event generator realization of our calculation in which realistic, finite p_T , $n(\gamma)$ radiation is incorporated in the production process on an event-by-event basis whereas the results in Ref. [3] are all semi-analytical. This enhances the significance of the general agreement of our results where they do overlap.

The issue of whether the calorimetric results are more realistic than the bare ones appears to depend on whether one is talking about the muon or the electron [22]. For the electron, it is very difficult to separate the soft photons with energy $\lesssim \Gamma_{M_W}$ that are responsible for the FSR effects of the W line shape as discussed already in Refs. [2, 3]; they are just a part of the electromagnetic calorimeter response in general that is used to measure the electron energy. For the muon, the energy is usually measured by a muon chamber in which in general these soft photons are not present. Thus, for the electron, our calorimetric results are more realistic; for the muon, it's the other way around. In either case, we see that precision W -pair production and decay studies need to take the interplay between the FSR and the EW corrections into account to obtain the most precise tests of the SM and our calculations in YFSWW3-1.12 afford an avenue to achieve that goal.

Acknowledgments

Two of us (S. J. and B.F.L. W.) acknowledge the kind hospitality of Prof. A. De Rujula and the CERN Theory Division while this work was completed. Two of us (B.F.L.W. and W.P.) acknowledge the support of Prof. D. Schlatter and the ALEPH Collaboration in the final stages of this work. One of us (Z.W.) acknowledges the support of the L3 group of ETH Zurich during the time this work was performed.

References

- [1] W. Beenakker et al., *WW Cross-Sections and Distributions*, in Reports of CERN Workshop "Physics at LEP2", edited by G. Altarelli, T. Sjöstrand, and F. Zwirner (CERN, Geneva, 1996), Yellow Report CERN 96-01, Vol. 1, p. 79.
- [2] W. Beenakker, F. A. Berends and A. P. Chapovsky, preprint hep-ph/9805327, May, 1998; Phys. Lett. **B435** (1998) 233.
- [3] W. Beenakker, F. A. Berends and A. P. Chapovsky, preprint hep-ph/9811481, November, 1998; preprint hep-ph/9902333, Feb., 1999.
- [4] S. Jadach, W. Płaczek, M. Skrzypek and B.F.L. Ward, Phys. Rev. **D54** (1996) 5434.
- [5] S. Jadach, W. Płaczek, M. Skrzypek, B.F.L. Ward and Z. Wąs, Phys. Lett. **B417** (1998) 326.

- [6] D. R. Yennie, S. Frautschi and H. Suura, *Ann. Phys.* **13** (1961) 379.
- [7] E. Barberio and Z. Wąs, *Comp. Phys. Commun.* **79** (1994) 291; and references therein.
- [8] See for example, G. Altarelli and G. Martinelli, in *Physics at LEP*, eds. J. Ellis and R. Peccei, (CERN, Geneva, 1986) p. 47; and references therein.
- [9] S. Jadach et al., to appear.
- [10] R. G. Stuart, *Phys. Lett.* **B262** (1991) 113; A. Aeppli, G.J. van Oldenborgh and D. Wyler, *Nucl. Phys.* **B428** (1994) 126.
- [11] K. Melnikov and O. Yakovlev, *Nucl. Phys.* **B471** (1996) 90.
- [12] W. Beenakker, F. A. Berends and A. P. Chapovsky, *Phys. Lett.* **B411** (1997) 203; *Nucl. Phys.* **B508** (1997) 17.
- [13] S. Jadach et al., *YFSWW3 1.12 MC Event Generator*, available from the authors at the WWW URL <http://enigma.phys.utk.edu/pub/YFSWW>.
- [14] A. Denner, S. Dittmaier and M. Roth, *Nucl. Phys.* **B519** (1998) 39; *Phys. Lett.* **B429** (1998) 145.
- [15] W. Beenakker *et al.*, *Nucl. Phys.* **B500** (1997) 255.
- [16] S. Jadach and B.F.L. Ward, *Phys. Rev. D* **38** (1988) 2897; *ibid.* **40** (1989) 3582; *Comp. Phys. Commun.* **56** (1990) 351.
- [17] J. Fleischer, F. Jegerlehner and M. Zralek, *Z. Phys.* **C42** (1989) 409;
M. Zralek and K. Kołodziej, *Phys. Rev.* **D43** (1991) 43;
J. Fleischer, K. Kołodziej and F. Jegerlehner, *Phys. Rev.* **D47** (1993) 830;
J. Fleischer *et al.*, *Comp. Phys. Commun.* **85** (1995) 29; and references therein.
- [18] M. Böhm *et al.*, *Nucl. Phys.* **B304** (1988) 463.
- [19] W. Beenakker *et al.*, *Phys. Lett.* **B258** (1991) 469; *Nucl. Phys.* **B367** (1991) 287.
- [20] S. Dittmaier, M. Böhm and A. Denner, *Nucl. Phys.* **B 376** (1992) 29; **B 391** (1993) 483 (E).
- [21] D. Yu. Bardin, S. Riemann, and T. Riemann, *Z. Phys.* **C32** (1986) 121; and references therein.
- [22] T. Kawamoto, private communication, 1998.

$$W^- \longrightarrow e^- \bar{\nu}_e$$

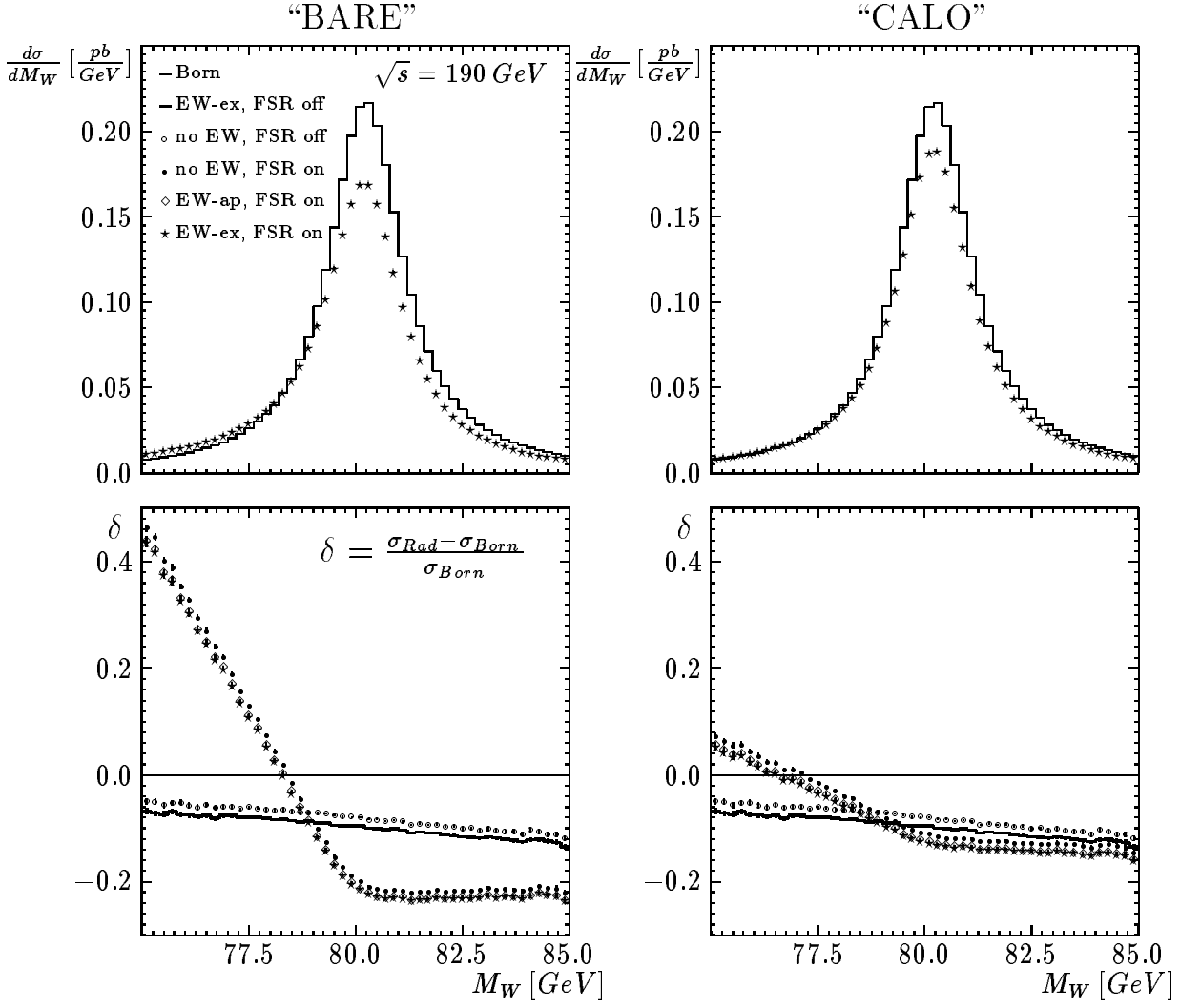


Figure 1: The W^- invariant mass distributions reconstructed from its decay products, $e^- \bar{\nu}_e$, four-momenta. In the left pictures the electron is treated exclusively ('bare' electron), while in the right pictures it is treated calorimetrically ('dressed' electron – its four-momentum is combined with four-momenta of all photons emitted within an angle of 5° around its direction). The input $M_W = 80.23 GeV$, $\Gamma_W = 2.034 GeV$.

$$W^- \longrightarrow e^- \bar{\nu}_e$$

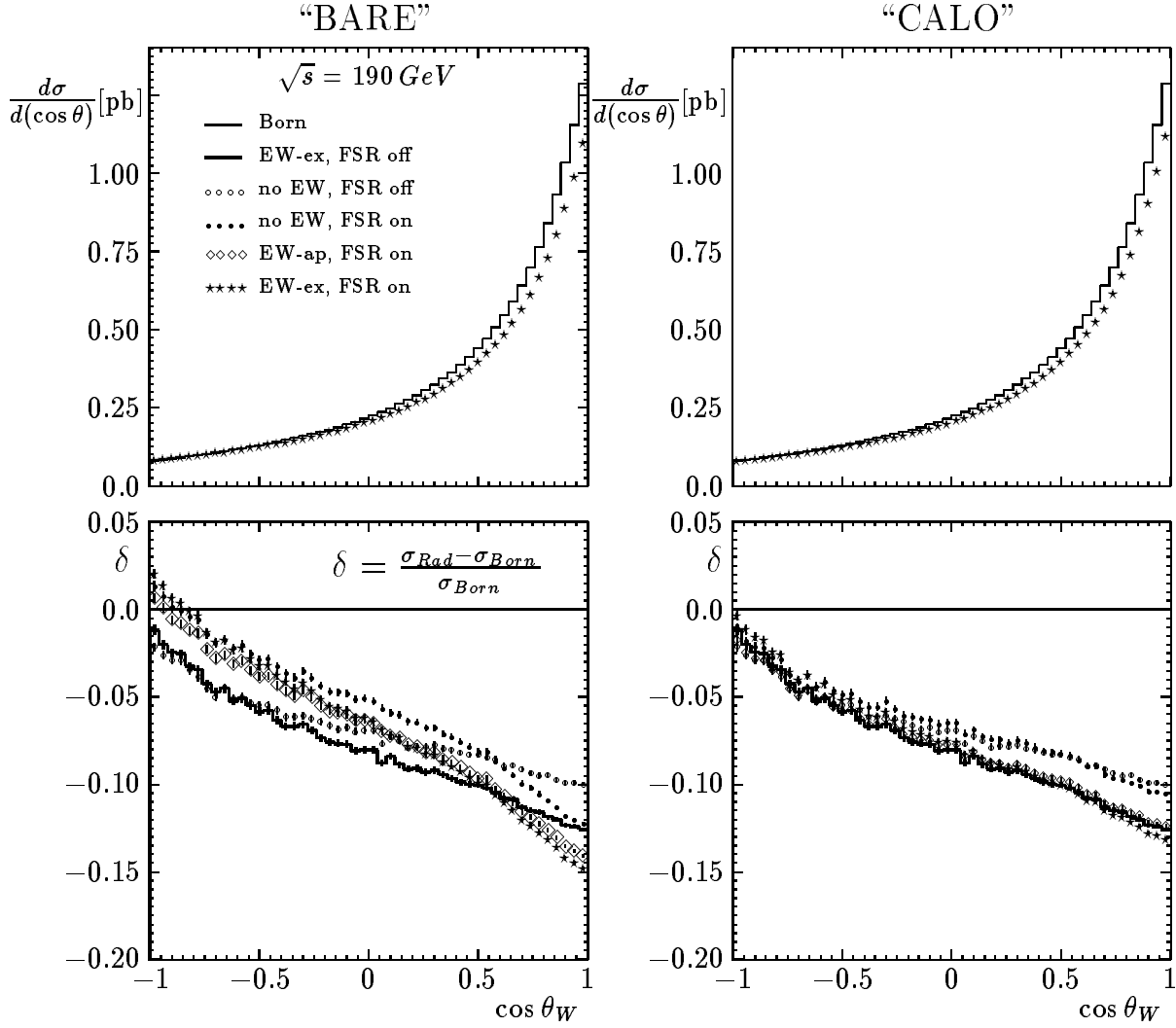


Figure 2: The W^- angular distributions reconstructed from its decay products, $e^- \bar{\nu}_e$, four-momenta. In the left pictures the electron is treated exclusively (‘bare’ electron), while in the right pictures it is treated calorimetrically as defined in Fig. 1.

$$W^- \longrightarrow e^- \bar{\nu}_e$$

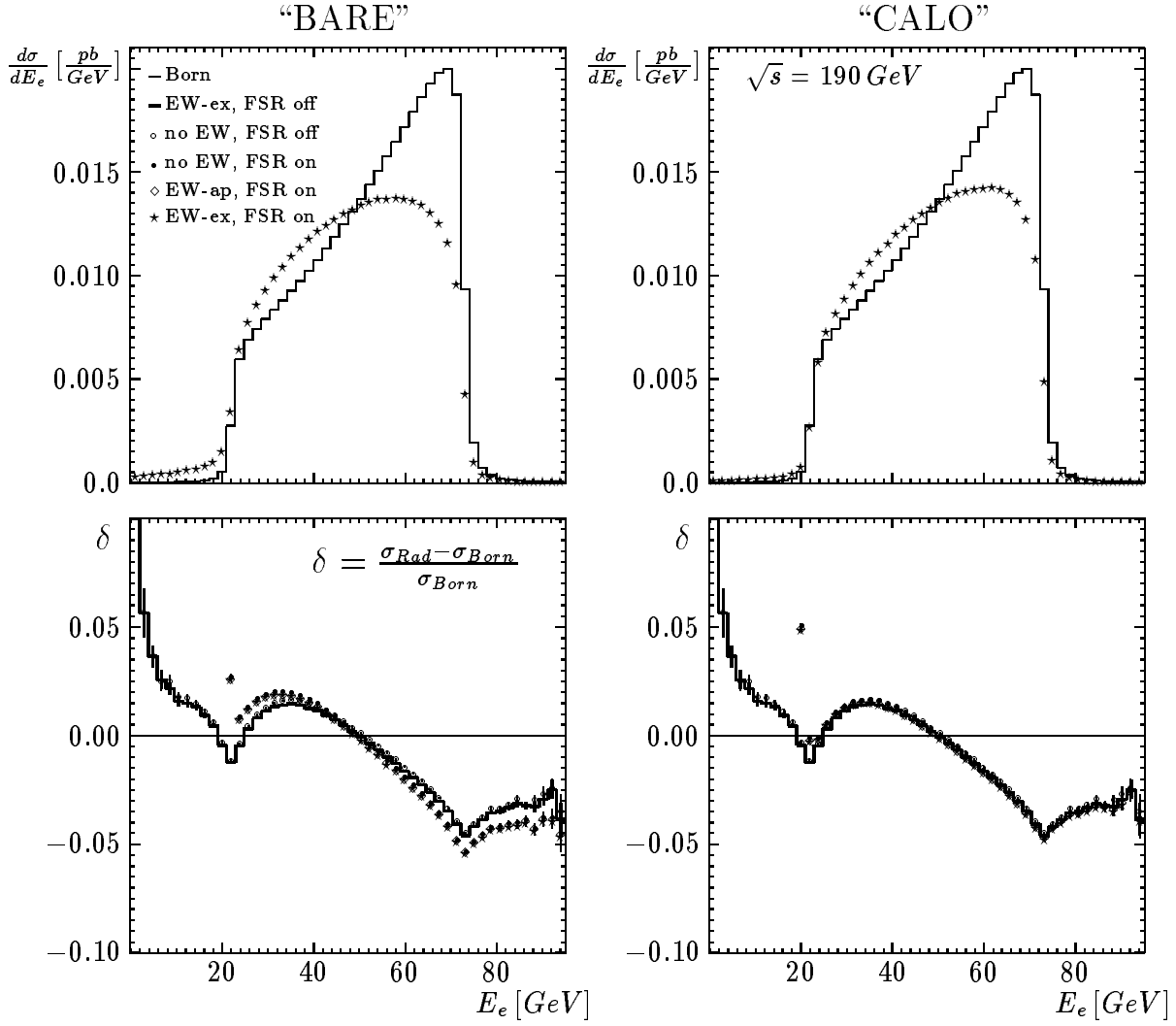


Figure 3: The distributions the final state electron energy in the LAB frame. In the left pictures the electron is treated exclusively ('bare' electron), while in the right pictures it is treated calorimetrically as defined in Fig. 1.

$$W^- \longrightarrow e^- \bar{\nu}_e$$

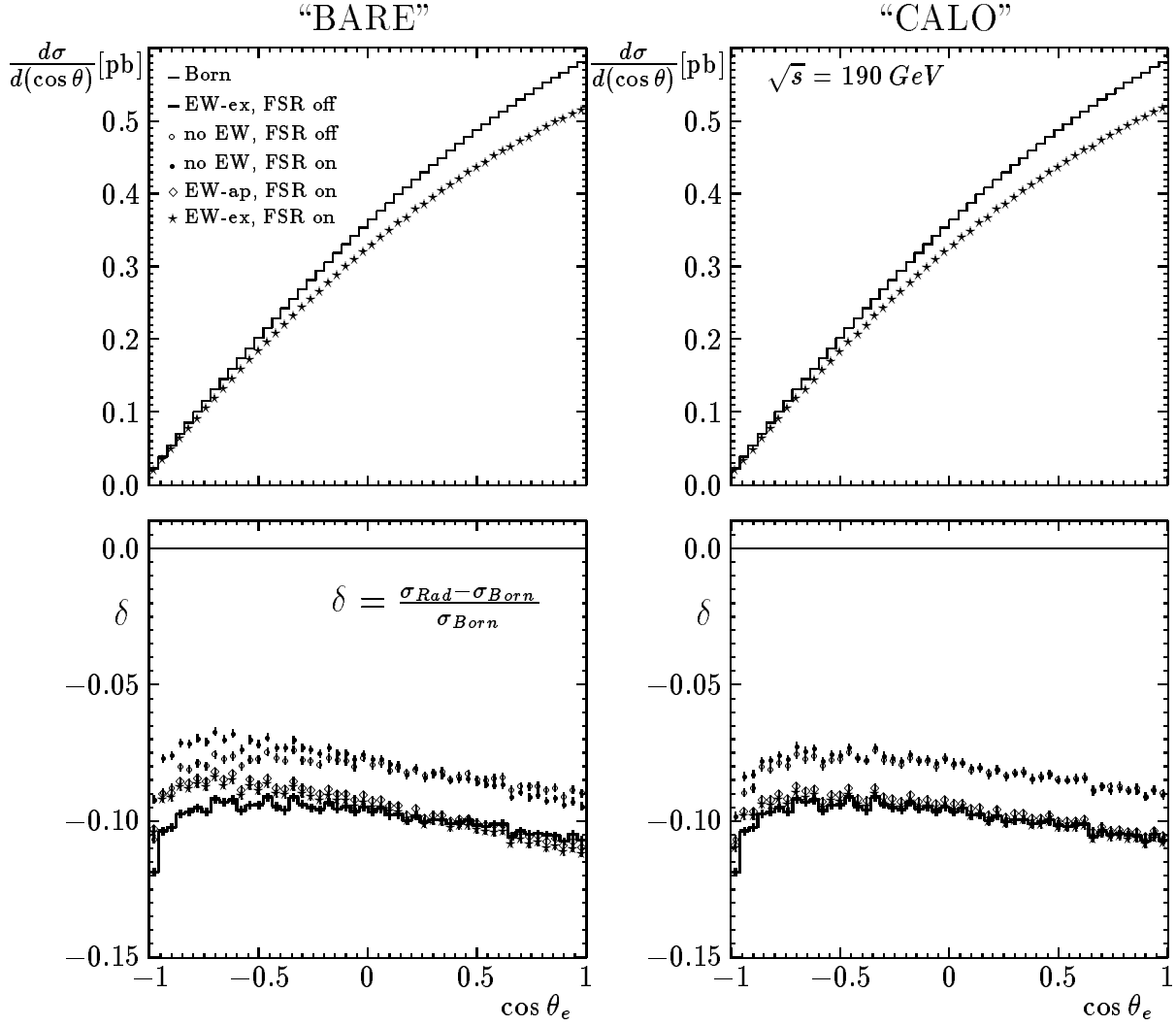


Figure 4: The distributions of the electron decay angle’s cosine in the W^- rest frame. In the left pictures the electron is treated exclusively (‘bare’ electron), while in the right pictures it is treated calorimetrically as defined in Fig. 1.

$$W^- \longrightarrow \mu^- \bar{\nu}_\mu$$

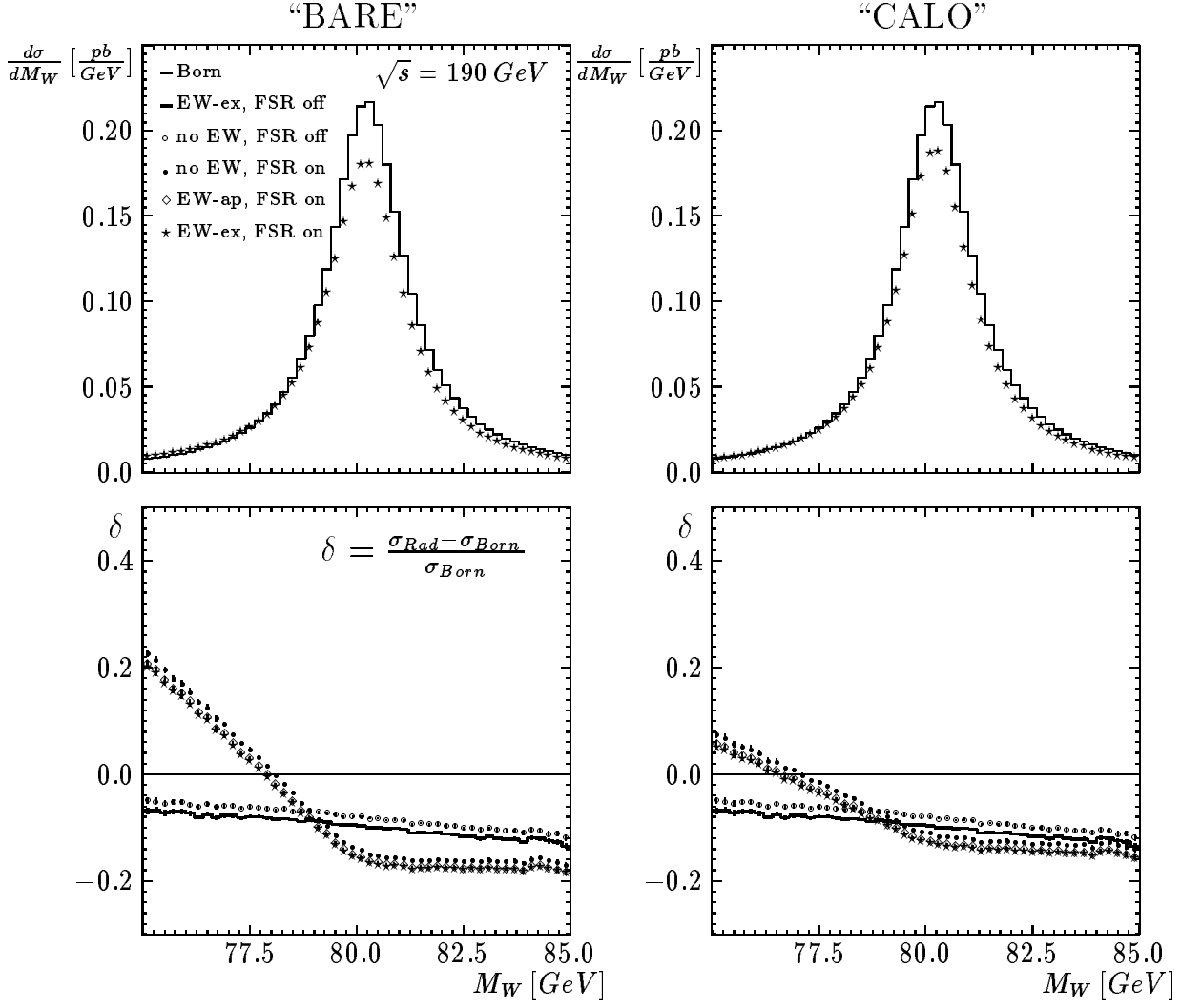


Figure 5: The W^- invariant mass distributions reconstructed from its decay products, $\mu^- \bar{\nu}_\mu$, four-momenta. In the left pictures the muon is treated exclusively ('bare' muon), while in the right pictures it is treated calorimetrically as defined in Fig. 1. The input $M_W = 80.23 \text{ GeV}$, $\Gamma_W = 2.034 \text{ GeV}$.

$$W^- \longrightarrow \mu^- \bar{\nu}_\mu$$

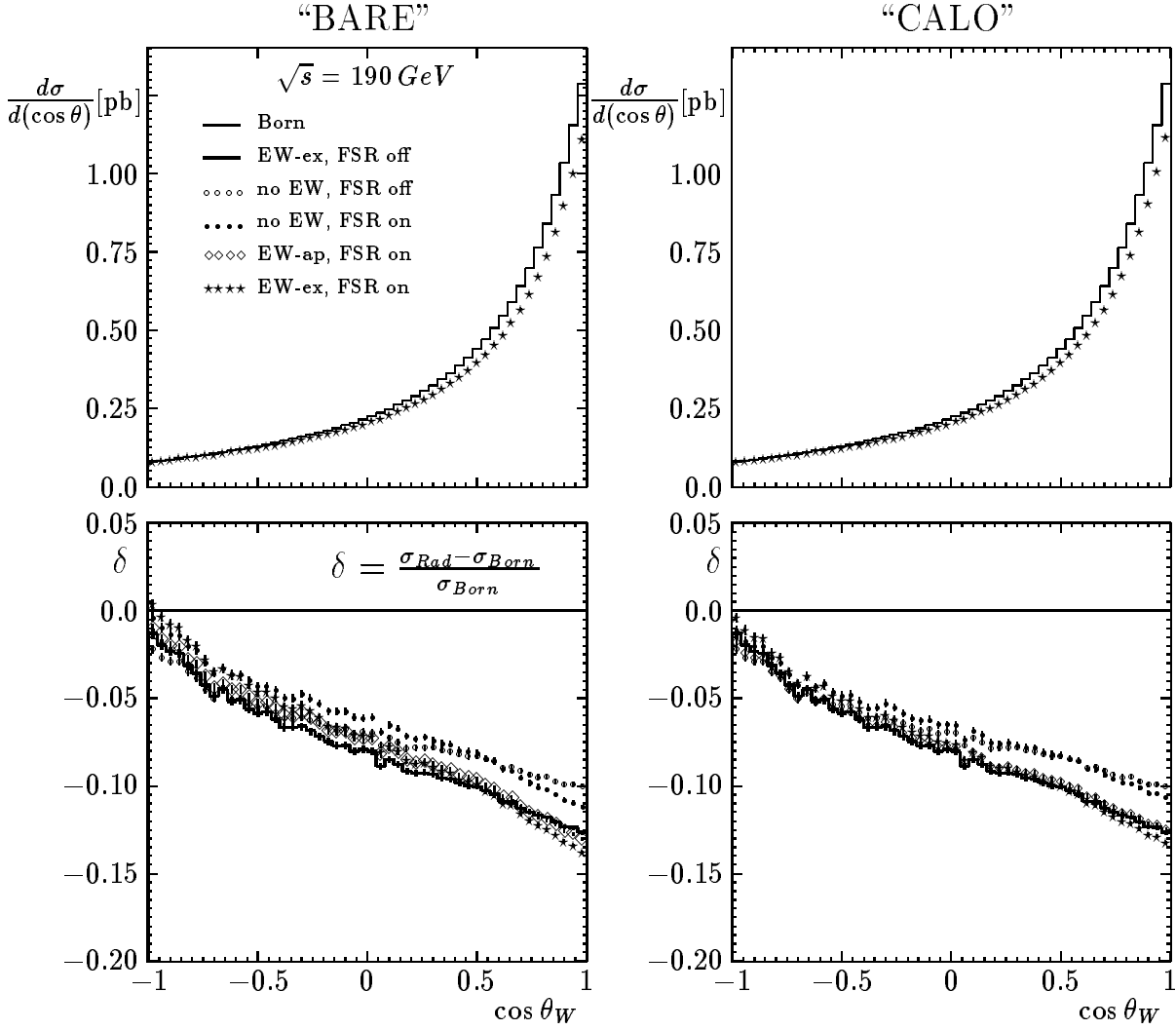


Figure 6: The W^- angular distributions reconstructed from its decay products, $\mu^- \bar{\nu}_\mu$, four-momenta. In the left pictures the muon is treated exclusively ('bare' muon), while in the right pictures it is treated calorimetrically as defined in Fig. 1.

$$W^- \longrightarrow \mu^- \bar{\nu}_\mu$$

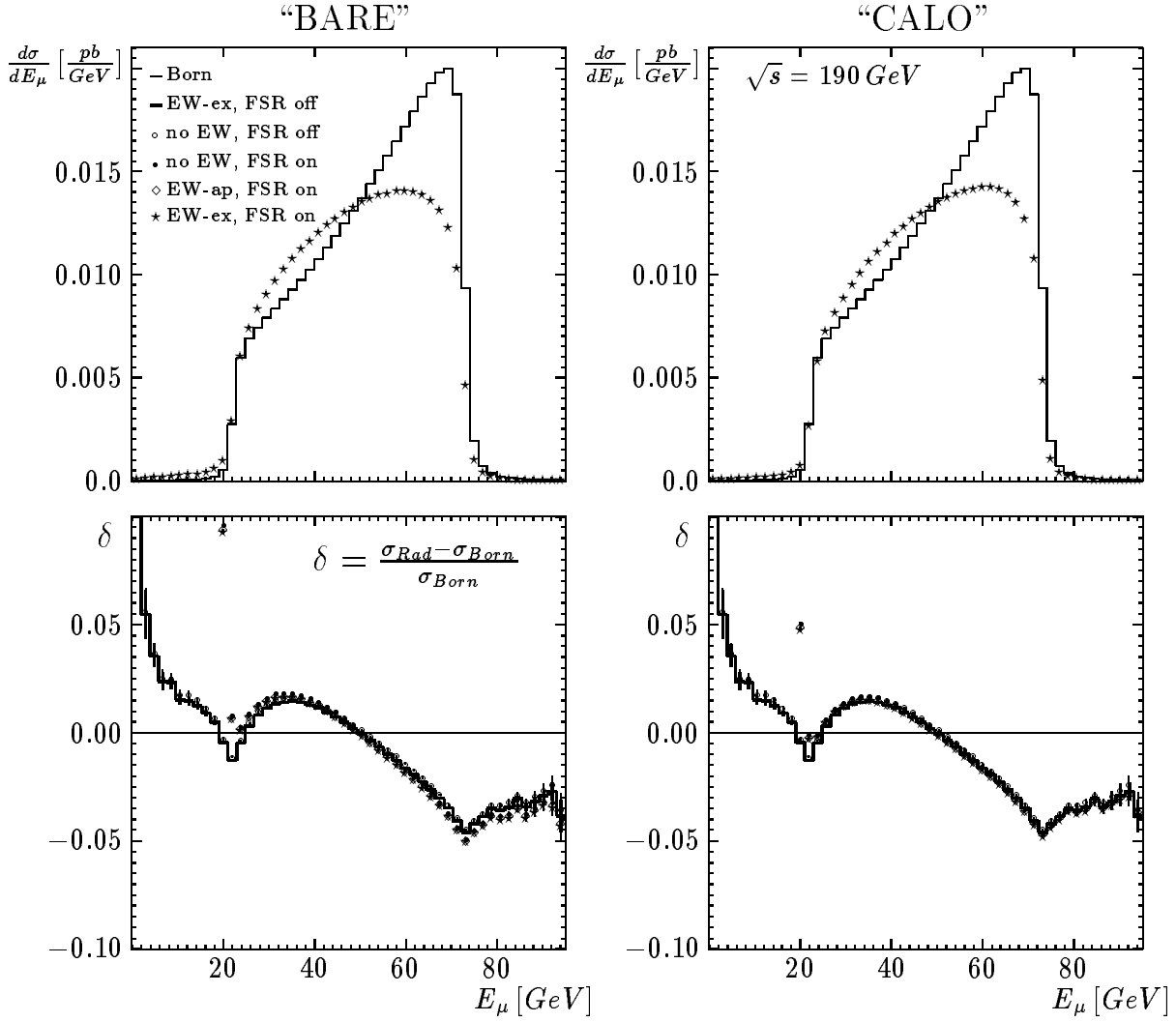


Figure 7: The distributions the final state muon energy in the LAB frame. In the left pictures the muon is treated exclusively ('bare' muon), while in the right pictures it is treated calorimetrically as defined in Fig. 1.

$$W^- \longrightarrow \mu^- \bar{\nu}_\mu$$

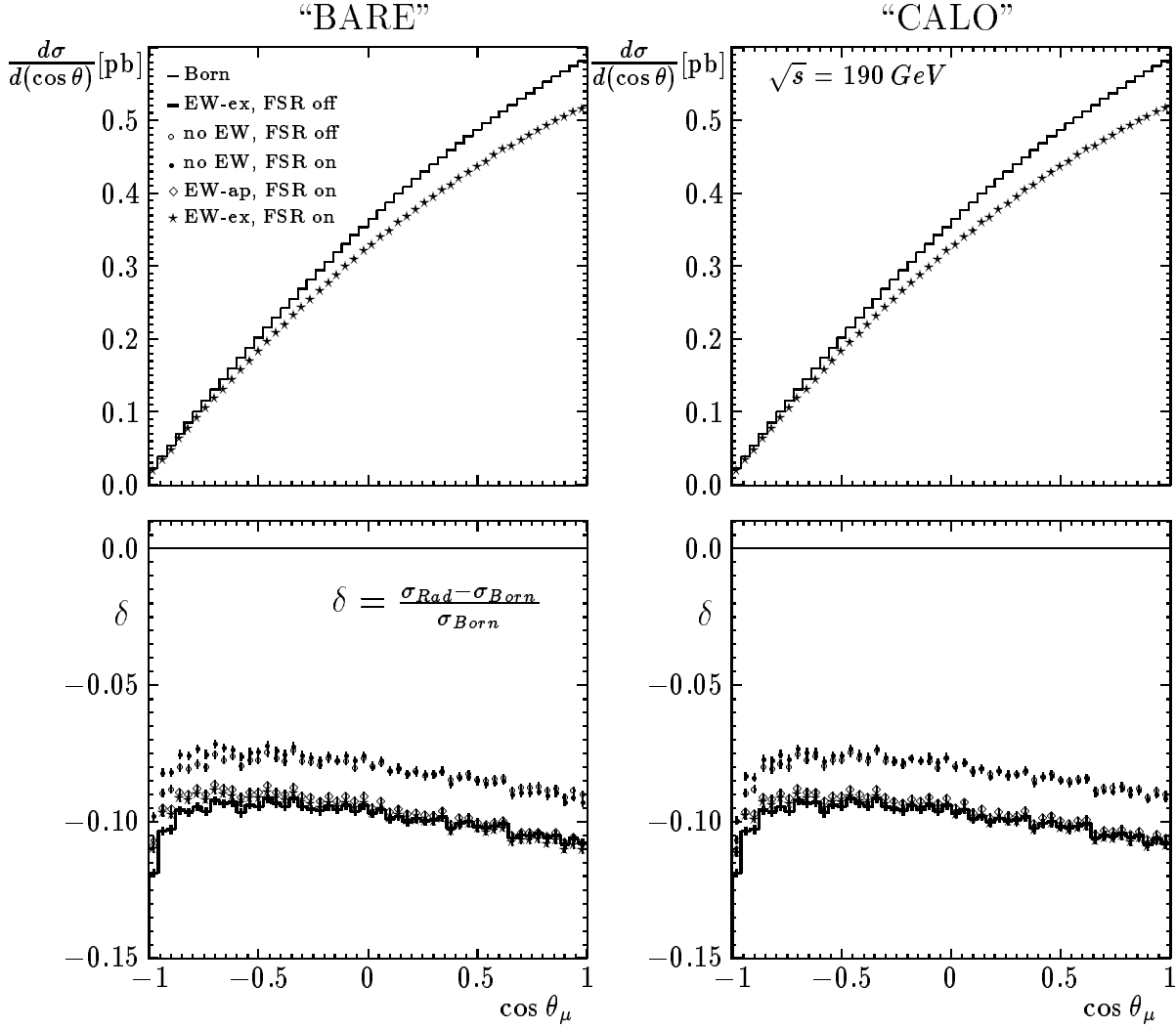
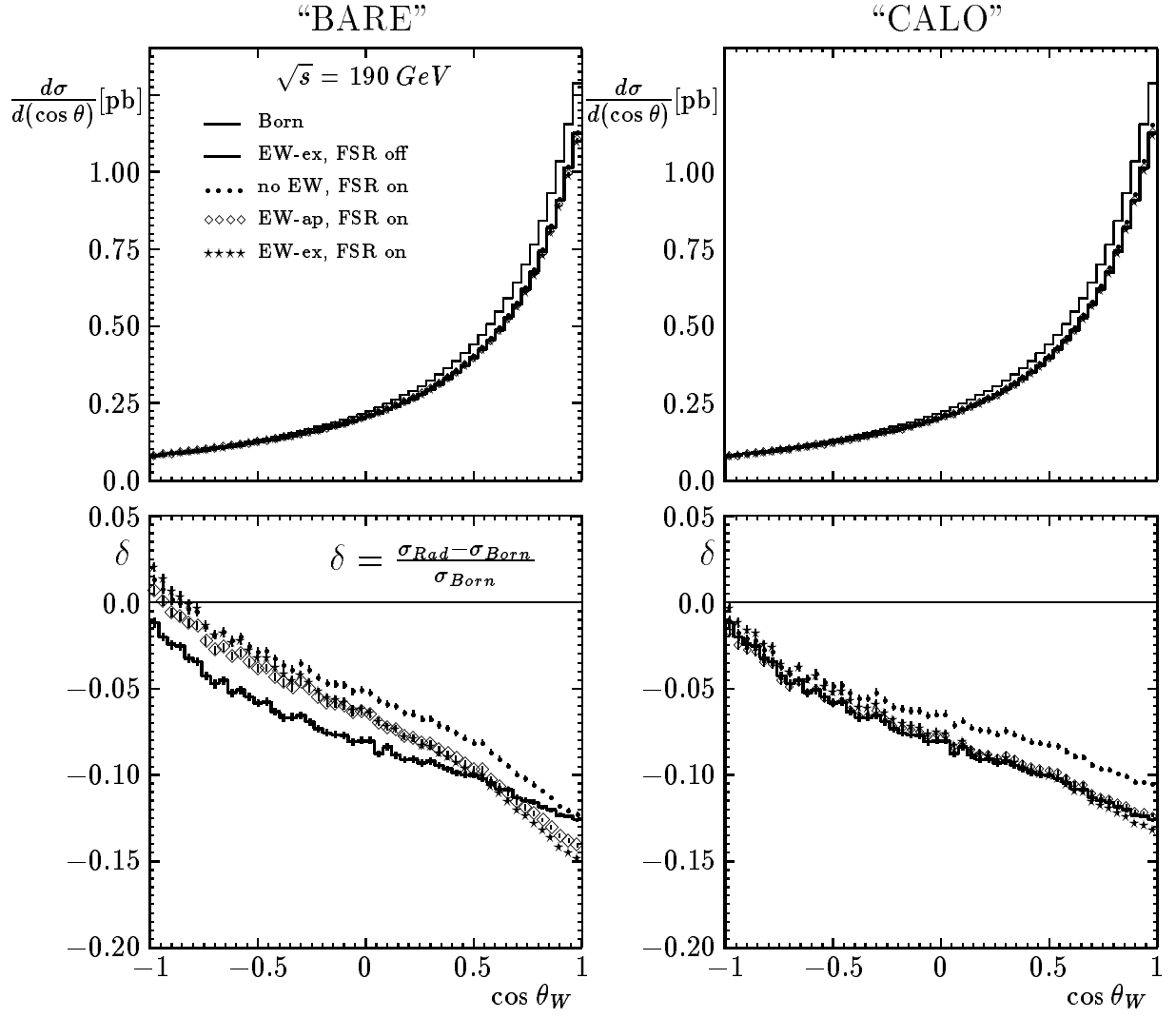
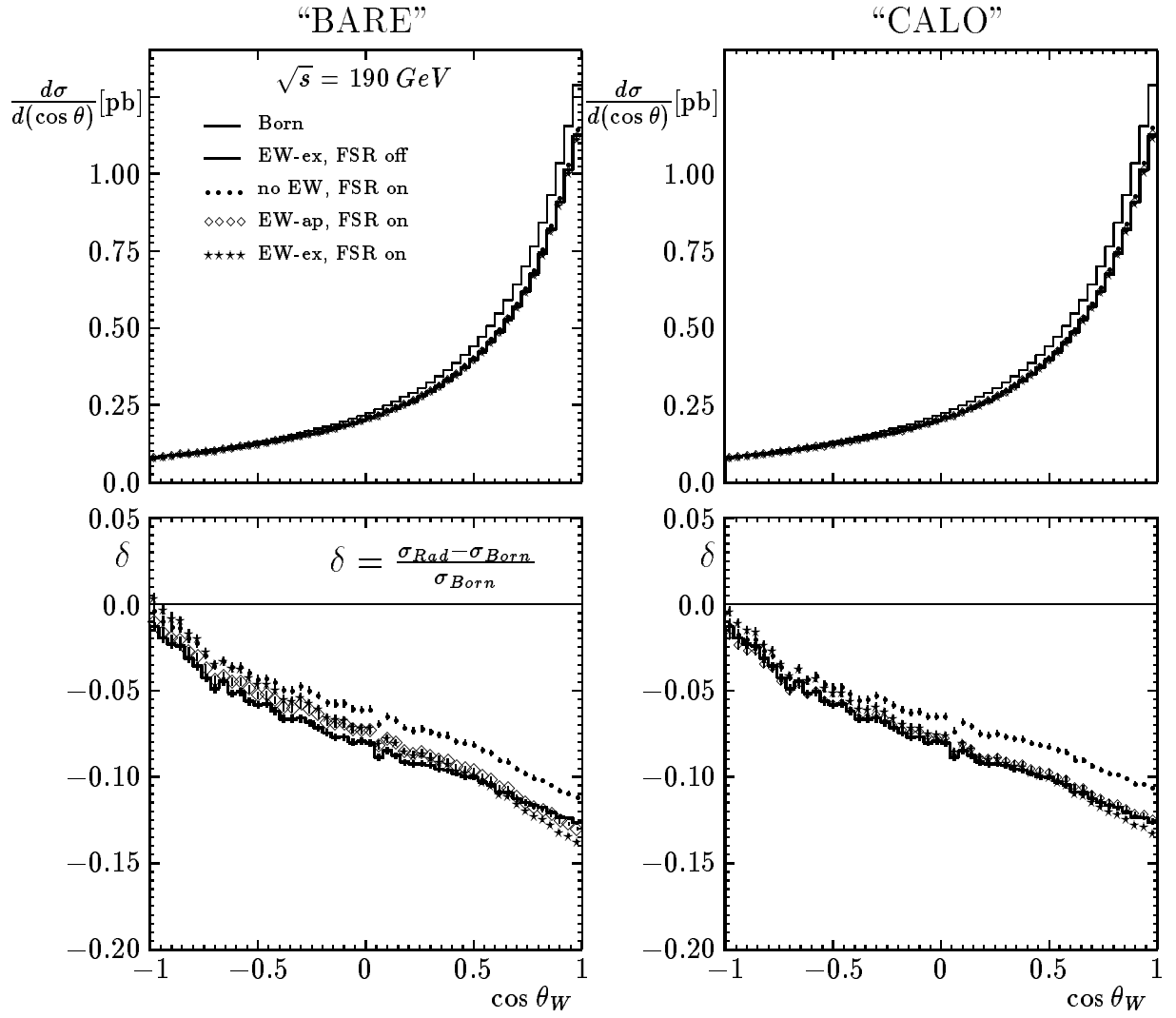


Figure 8: The distributions of the muon decay angle's cosine in the W^- rest frame. In the left pictures the muon is treated exclusively ('bare' muon), while in the right pictures it is treated calorimetrically as defined in Fig. 1. 5° around its direction).

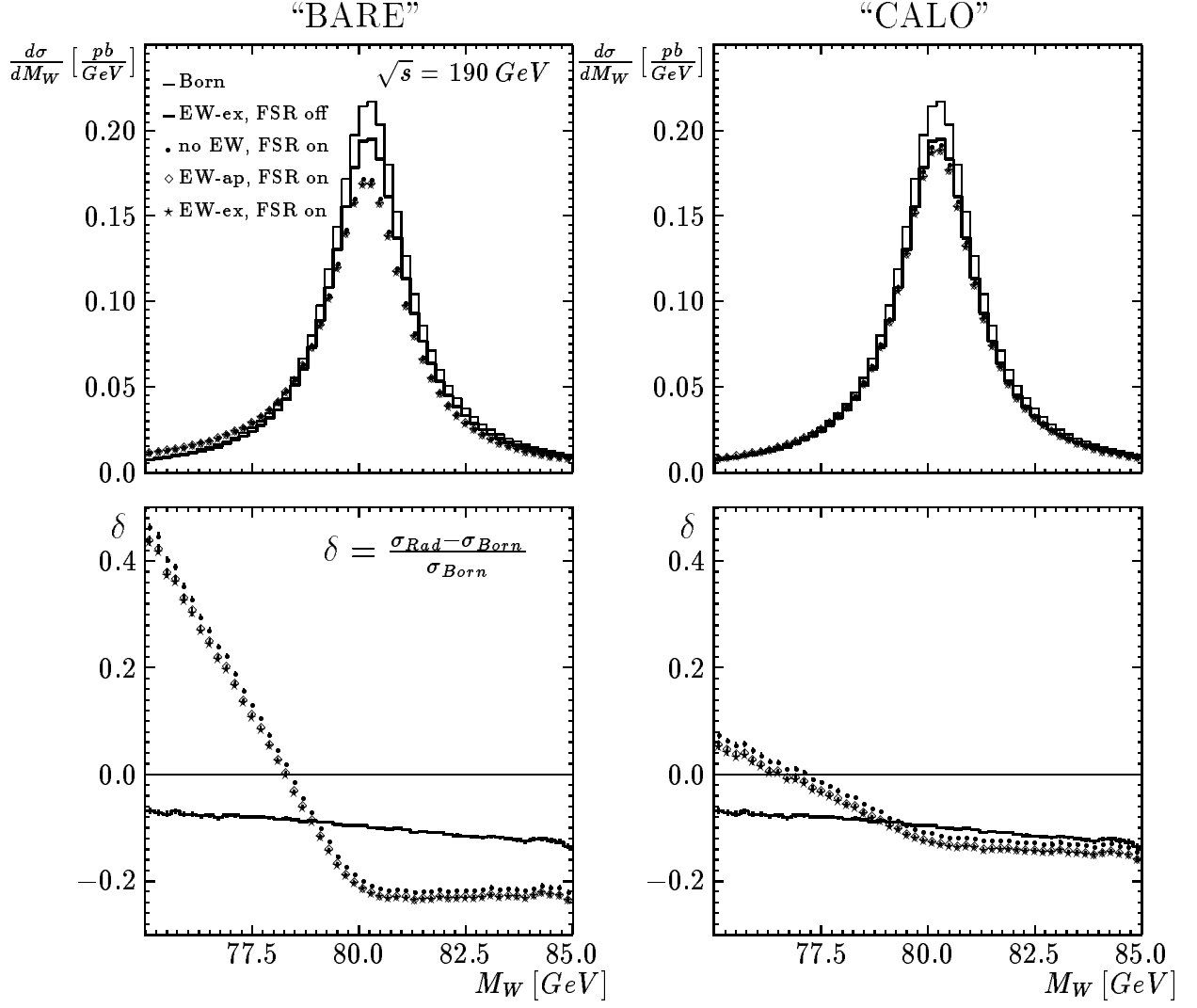
$$W^- \longrightarrow e^- \bar{\nu}_e$$



$$W^- \longrightarrow \mu^- \bar{\nu}_\mu$$



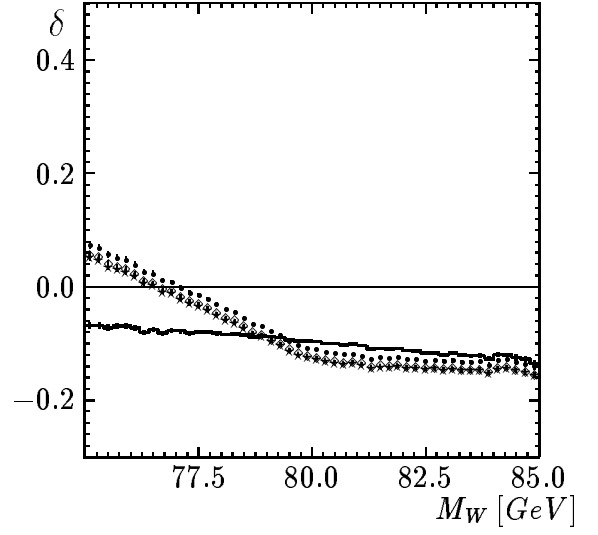
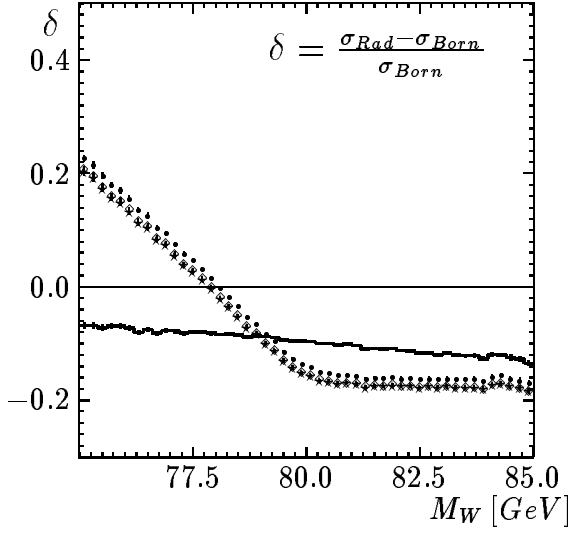
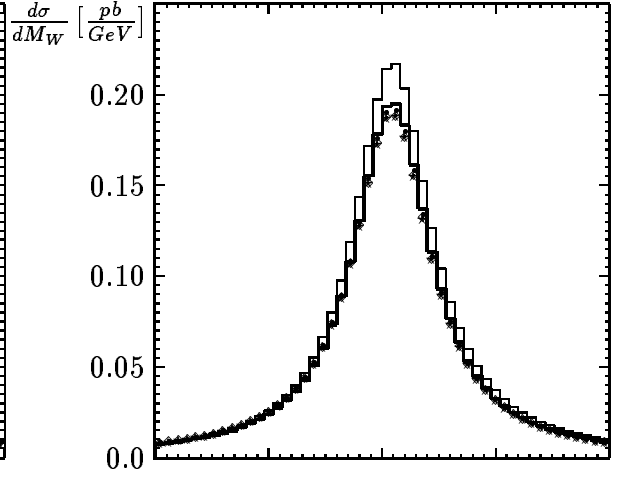
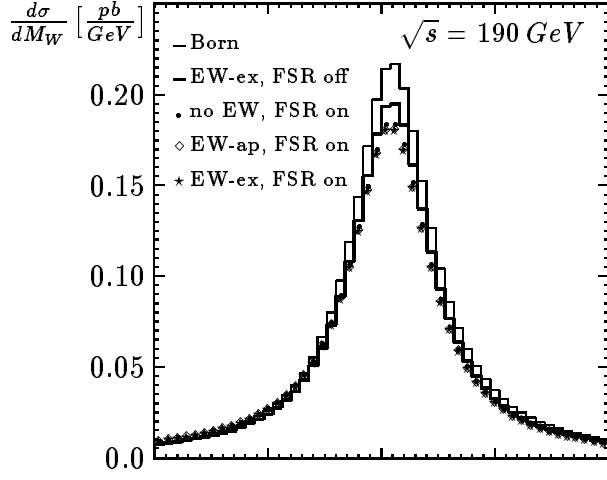
$$W^- \longrightarrow e^- \bar{\nu}_e$$



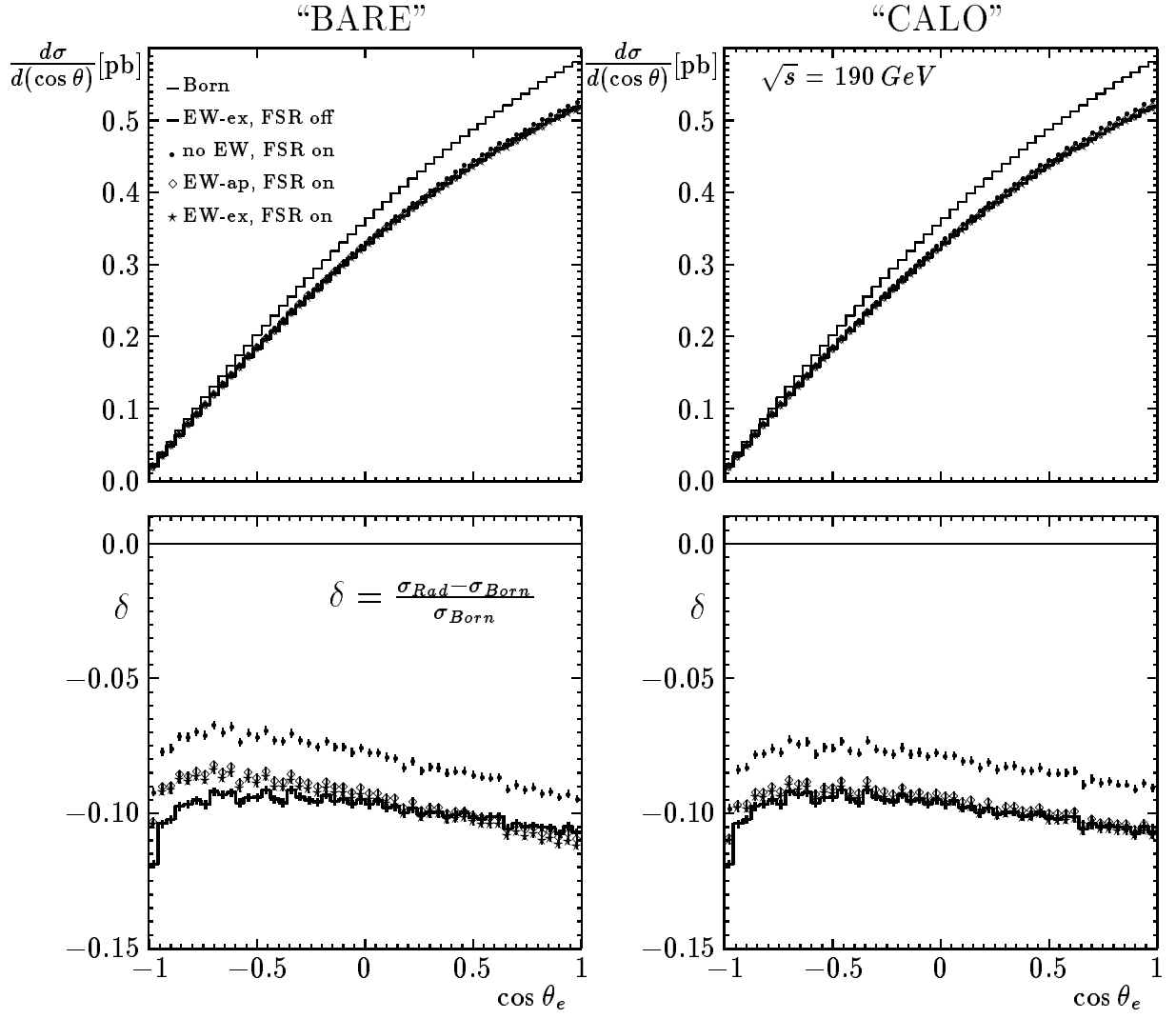
$$W^- \longrightarrow \mu^- \bar{\nu}_\mu$$

“BARE”

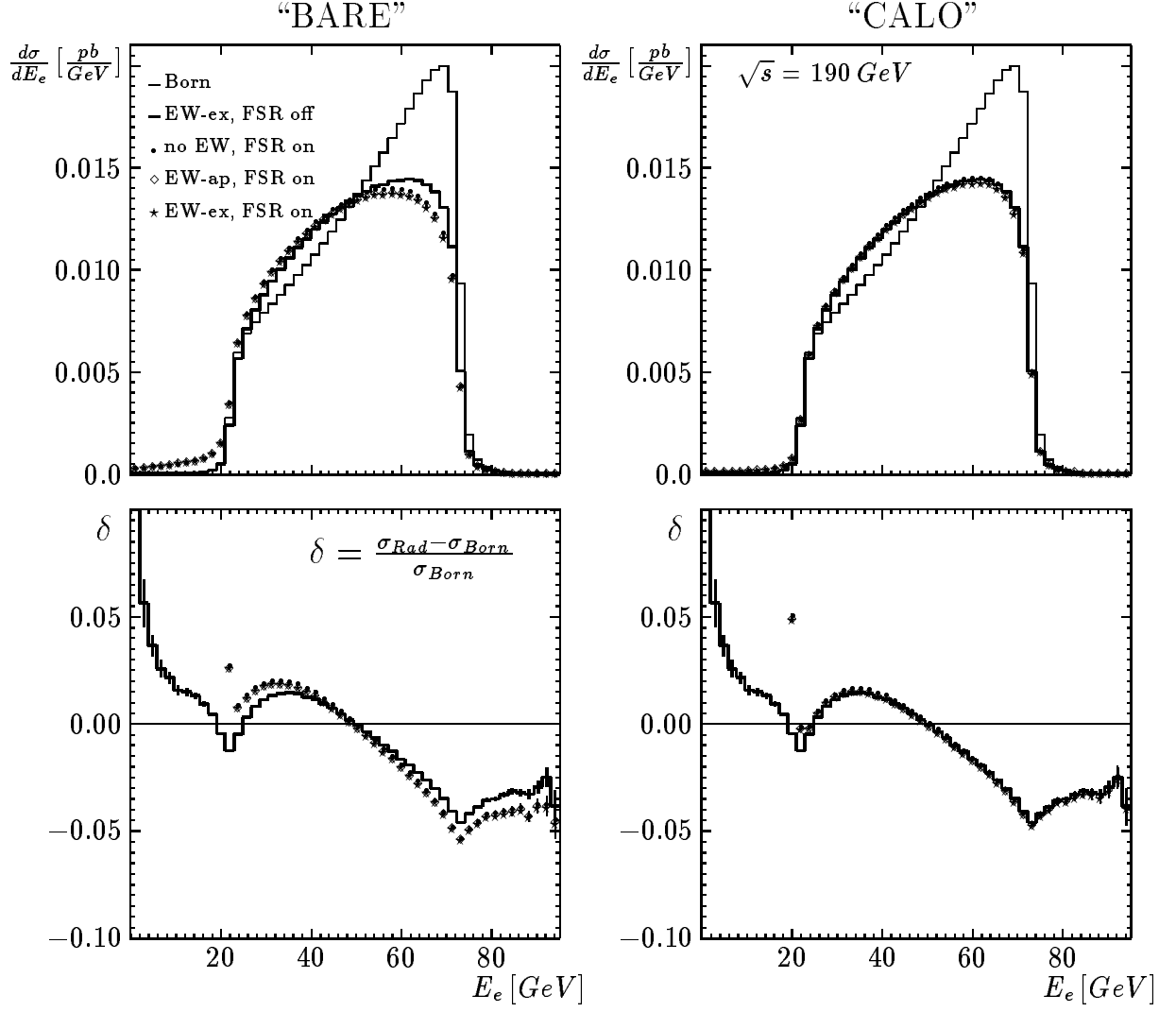
“CALO”



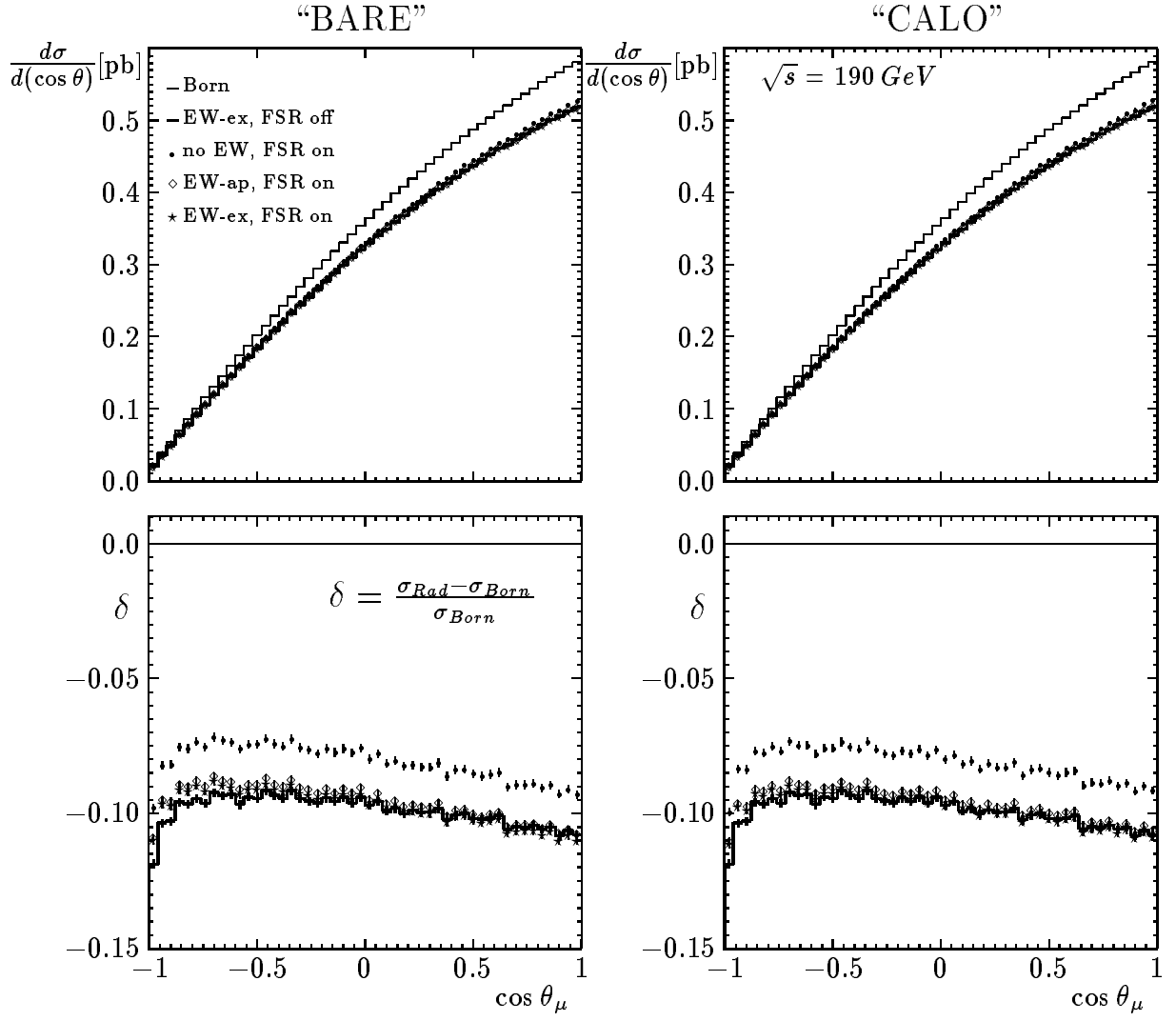
$$W^- \longrightarrow e^- \bar{\nu}_e$$



$$W^- \longrightarrow e^- \bar{\nu}_e$$



$$W^- \longrightarrow \mu^- \bar{\nu}_\mu$$



$$W^- \longrightarrow \mu^- \bar{\nu}_\mu$$

